Contactless Electrical Characterization of HEMT Epitaxial Structures and Devices

S.Solodky[1], T.Baksht[1] , A. Kramtsov[2], I. Ortenberg[1], M. Vazokha[1], M.Leibovitch[3], A. Hava[2] and Yoram Shapira[1]

[1]Department of Electrical Engineering - Physical Electronics, Tel-Aviv University, Ramat-Aviv 69978, Israel

phone: 972-3-6408015 e-mail: sana@eng.tau.ac.il

[2] Dep. Of Electrical And Computer Engineering, Ben-Gurion University, Beer-Sheva

[3]Gal-El (MMIC), P.O. Box 330, Ashdod 77102, Israel

Keywords: GaN HEMT, PHEMT, MHEMT, contactless characterization

Abstract

AlGaN/GaN HEMT, AlGaAs/InGAs/GaAs PHEMT and InAlAs/InGaAs MHEMT epitaxial structures have been characterized using surface photovoltage spectroscopy. The effects of the transistor top and bottom delta-doping levels $?_{top}$, $?_{bot}$ and surface charge Q_{sur} on the spectrum features have been studied using numerical simulations. Universal empirical model has been developed, which allows extraction and comparison of $?_{top}$, $?_{bot}$ and Q_{sur} and is applicable for both double-sided and single sided delta-doped structures. Effect of GaN HEMT surface passivation has been studied. Prediction of the final device performance by the model is shown for two MHEMT structures. Correlation between extracted *Qsur* and device pinch-off voltage *Vp* is shown.

INTRODUCTION

GaN/AlGaN HEMTs have been very promising for high power high-speed applications[1] due to their high electron mobility of two dimensional electron gas (2DEG), good thermal isolation and high breakdown voltage. High cutoff and maximum oscillation frequencies[2,3] together with low-cost GaAs substrates make MHEMTs attractive for low-noise applications. InGaAs/GaAs PHEMTs are "working horses", widely used for microwave, high speed and power applications.[4]

The interplay of epitaxial structure parameters and lateral geometry parameters of a transistor defines the distribution of electric fields within the device and thus its electrical performance. The top and bottom delta-doping levels, $?_{top}$ and $?_{bot}$, together with the surface and interface charge densities Q_{sur} and Q_{int} and layer thickness define the distribution of the vertical electric fields within the device and the electron sheet density in the channel. They affect the final DC and RF device parameters. Thus, it is crucially important to develop a methodology capable of predicting eventual device performance based on monitoring epi-structure parameters. Such a methodology should be contactless, nondestructive, wafer-scalable and usable for structures with different material compositions. Indeed, photoluminescence[5,6] electroreflectance, photoreflectance[7] and X-ray microscopy[8] have been used for the characterization of HEMT structures.

Surface photovoltage spectroscopy (SPS) is a method, which fulfills most of the demands for comprehensive transistor structure characterization and for incoming wafer inspection.[9] SPS monitors changes in the semiconductor surface work function induced by absorption of monochromatic light, giving rise to surface photovoltage (SPV). A detailed description of this method and its applications may be found in Ref. [10]. This technique has been successfully applied for characterization of novel structures and devices.[11-15]

In this work, HEMT structures have been characterized using SPS measurements and numerical simulations. We introduce an empirical model, which correlates spectral features and epitaxial structure parameters. Applying the empirical model to MHEMT and PHEMT structure analysis shows the universality of the model for different HEMT structures. We show examples of the model application to comparison of GaN HEMT, PHEMT and MHEMT epitaxial structures before and after processing. DC measurements performed on complete devices show correlation between epi-structure parameters and final device performance.

EMPIRICAL MODEL

HEMT structures have been fabricated by metal-organic chemical vapor deposition (MOCVD) and molecular beam epitaxy (MBE) growth techniques. Table I summarizes the material composition and range of doping levels of the structures as given by manufacturer. SPS experiments have been performed in air using a commercial Kelvin probe unit with a sensitivity of ~1 mV.

TABLE I.

MATERIALS PROPERTIES OF STUDIED HEMT STRUCTURES

	PHEMT	**MHEMT**	**AlGaN/GaN HEMT**
Growth technique	MBE	MBE	MOCVD
Substrate	GaAs	GaAs	SiC
Channel	$In_{0.2}Ga_{0.8}As$	$In_{0.5}Ga_{0.5}As$	GaN
Buffer	GaAs-AlGaAs	InAlAs	GaN
Schottky layer	AlGaAs	InAlAs	AlGaN
$?_{top}$	3-6x10^{12} cm^{-2}	3-6x10^{12} cm^{-2}	1x10^{13} cm^{-2}
$?_{bot}$	0.4-1.5x10^{12} cm^{-2}	0.4-1.5x10^{12} cm^{-2}	-

The total SPV signal is a combination of the signals from all structure layers. The signal magnitude is a complicated function of light absorption and the electric fields in any absorption region. Absorption of light in the quantum well (QW) creates electron-hole pairs. While electrons are confined within the QW by fields in buffer and Schottky layer, holes are likely to overcome the QW-Schottky layer interface or the QW-buffer interface potential barrier. The holes are swept by the electric field in the buffer or in the Schottky layer direction, contributing to signals with opposite signs. The inset in Fig. 1 shows the simulated SPV signal from the buffer (circles), the Schottky layer (squares) as well as the total signal (solid curve) for a double-sided delta-doped PHEMT structure. In the simulated case, at photon energies below 1.37 eV the signal from the buffer is dominant, which results in a positive total SPV. When the signal from the buffer is saturated, the total SPV changes sign because of the dominating signal from the Schottky layer. The absorption in the buffer is the reason for the second peak formation. In a singe sided delta-doped HEMT structures, a triangular QW is formed at the interface with Schottky layer. Thus, the potential barrier for holes is much smaller in the Schottky layer direction and holes generated by QW absorption are swept toward the Schottky layer, contributing to a dominant positive signal in the QW region of absorption.

Figure 1 shows parts of SPV spectra of a double-sided delta-doped PHEMT structure (solid curve) and two MHEMT structures, M1 (circles) and M2 (squares), which differ in their top delta-doping $?_{top}$ levels. Differences in $?_{top}$ between the structures lead to changes in electric fields distributions and potential profiles, which, in turn, lead to variations of spectral shapes between the structures. At the low energy region, absorption takes place in the QW. At this portion of the spectrum, increasing signals (for PHEMT and M2 spectra) as well as decreasing signals (for M1) are observed. At energies above 1.4 eV, a second peak in the PHEMT spectrum is observed. This feature may be attributed to GaAs absorption. At low photon energies, Fermi filling, due to high electron concentration in the channel, dominates the InGaAs absorption coefficient.[16] This effect significantly changes the absorption coefficient of the QW by blue shifting its edge and reducing its magnitude at higher energies.

Figure 2 shows SPV spectra of a single-sided delta-doped GaN HEMT before SiN passivation (solid line), after SiN passivation (circles) and a MHEMT (see inset of Fig. 2). The total signal in the QW absorption region is positive. Therefore, SPV spectra of double-sided and single-sided delta-doped structures with different material composition may be fully understood.

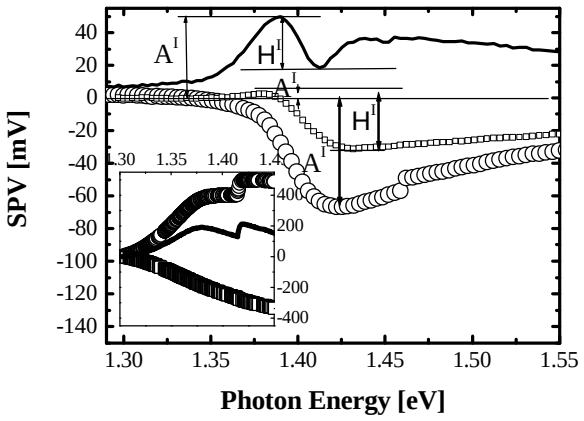

Figure1. Typical surface photovoltage spectra of a PHEMT (solid curve) and two MHEMT structures: M1 (circles) and M2 (squares). Labels correspond to the spectrum parameterization scheme: A^I-amplitude of the first peak, H^I-first peak height. Inset: Simulated SPV signal from a double-sided delta-doped PHEMT structure (solid curve) together with simulated signals from buffer (circles) and Schottky layer (squares).

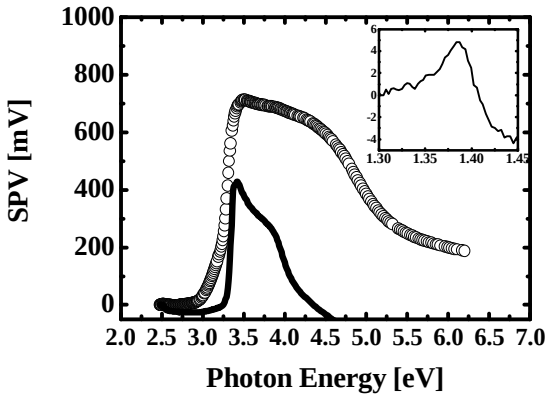

Figure2. SPS spectra single-sided doped structures – GaN HEMT before SiN passivation (solid line), GaN HEMT after passivation (circles) and MHEMT (inset).

The spectra of HEMT structures were parameterized (See Fig. 1). The spectral parameters are the amplitude of the first peak (or minimum) A^I and the peak height H^I. The empirical model, which correlates between the spectral features A^I, H^I and the structural parameters $?_{top}$, $?_{bot}$ and $Q_{sur,}$ has been developed using numerical simulations. This model has been applied to several PHEMT structures and the efficiency of the model for PHEMT characterization is shown in [15]. The model shows that the differences in a spectral parameter A^J (relative to a reference structure) is given by:

$$? A^J(?_{top,} ?_{bot\,,} Q_{sur}) = C_{?top}? ?_{top}+C_{?bot}? ?_{bot}+C_{Qsur}? Qs_{ur}, \quad (1)$$

where $C_{?top}$, $C_{?bot}$, C_{Qsur} are coefficients, which weight the influence of each of the electrical parameters on the spectral parameter A^J.

RESULTS

Spectra of double-sided delta-doped PHEMT (represented by the solid curve in Fig. 1) and MHEMT (dotted curve) were compared. The $?_{top}$ in the PHEMT structure is $5x10^{12}$ cm^{-2}. The structures have the same $?_{bot}$ level and the difference in $?_{top}$ specified by the supplier is $1x10^{12}$ cm^{-2}. Variations in $?_{top}$ change the electric field distribution in the Schottky layer region and thus the spectral shapes of the QW absorption region significantly differ. The difference in $?_{top}$ has been calculated using the model. Q_{sur} is assumed to be the same, which reduces eq. (1) to $? A^I= 130? ?_{top}$. The calculated $? ?_{top}$ is $0.9x10^{12}$ cm^{-2}, which is in good agreement with the grower specifications. Two single-sided top-delta-doping structures of not passivated GaN/AlGaN HEMT and MHEMT have been compared using the empirical model. In these HEMTs, $?_{top}$=$1.0x10^{13}$ cm^{-2} and $0.6x10^{13}$ cm^{-2}, respectively. The value of $? ?_{top}$ calculated from the model is $4.4x10^{12}$ cm^{-2}, which is in good agreement with the supplier specifications.

Therefore, the model developed for double-sided delta-doped PHEMT structures accounts well for differences in $?_{top}$ of GaN HEMT and MHEMT structures. This model is applicable for double-sided delta-doped as well as for single-sided delta-doped structures. It shows that this is a universal empirical model, sensitive to differences in doping levels for a wide variety of HEMT structures.

Surface passivation of HEMT structures significantly affects the device performance.[17] That is why it is crucially important to study its influence on device surface. Figure 1 shows SPV spectra of a HEMT structure before (solid curve) and after (circles) SiN passivation. Applying the model for comparison of the two spectra yields a numerical value of $? Q_{sur}$=$1.8x10^{12}$ cm^{-2}. It means that SiN passivation reduces surface charge density. In addition, the signal drop of the AlGaN in the passivated structure starts at higher energy values. This is probably because of passivated surface states present in the AlGaN prior to SiN deposition.

The model has been applied to the two double-sided delta-doped MHEMT structures, M1 and M2, whose spectra are shown by the circles and squares, respectively in Fig. 1. There is a difference in the $?_{top}$ level between the two structures, denoted by $? ?_{top}$. A higher $?_{top}$ in M2 leads to the dominating signal from its buffer layer and an overall positive signal in the QW region. The $?_{top}$ of M1 is $4.45x10^{12}$ cm^{-2}. The $? ?_{top}$ extracted from the model is $0.5x10^{12}$ cm^{-2}, which is in good agreement with the grower specifications that are $0.55x10^{12}$ cm^{-2}.

In order to check the robustness of the model in wafer incoming inspection, the 0.25 ?m devices have been fabricated on wafers with epi-structures similar to M1 and M2 structures. The device characteristics related directly to the delta-doping level is the maximum drain–source current - I_{max}. Imax is defined as the drain current at maximum gate voltage. This current is given by the expression:

$$I_{max}=qn_sv_sw \quad (2),$$

where q is the electron charge, n_s- the channel electron sheet density, v_s- the electron saturation velocity in the channel and w- is the gate width. Thus, for devices with the same gate periphery (w), Imax is defined by n_S, which is given by:

$$n_s ? ?\int_{x_1}^{x_2} n(x)dx \quad (3)$$

where $n(x)$ is the distribution of mobile charges within the well, x_1 and x_2 are the coordinates of the buffer/QW and the QW/Schottky layer interfaces, respectively[18]. n(x) is related directly to the delta doping levels.

Id (Vgs) curves for transistors with 100 ?m gate periphery fabricated on M1 (circles) and M2 (squares) structures measured at a drain-source voltage of Vds=1Vhave been measured. Table II summarizes the results of comparing two epi-structures and fabricated devices. The results show a good correlation between supplier data, differences in *?top* extracted from the model and final device performance. This demonstrates the sensitivity of our methodology to even slight differences in the delta-doping level and allows prediction of the device DC and power performance.

Two MHEMT wafers W1 and W2 with same epitaxial structure before the fabrication process have been characterized using SPS after fabrication. Applying the model to comparison of the two spectra allowed extraction of *? Qsur* between the two structures. It shows a more positive surface charge at W1 by $5.6x10^{12}$ cm^{-2}.

According to the linear charge control model, [18] the device pinch-off voltage *Vp* is proportional to the doping density. More positive surface charge means increased effective doping density. It leads to a more negative Vp and higher drain currents. In order to prove the correlation between the surface charge extracted from SPS measurements and device performance, identical coplanar devices with 200 ?m gate periphery have been characterized and compared on W1 and W2.

TABLE II.

RESULTS OF SPS AND DC CHARACTERIZATION OF M1 AND M2

?top for MHEMT structure M1 [$X10^{12}cm^{-2}$]	4.45
Relative *?? ?top* by supplier [%]	12
Relative*?? ?top* from model [%]	11
Relative *? ?max* calculated [%]	12

Results of device comparison on W1 and W2 are shown in Table III. The results show a higher drain saturation current - *Idss*, and a more negative pinch-off voltage *Vp* for wafer W1. Thus, SPS may be used as a characterization technique that is sensitive not only to epitaxial structure parameters but to final device performance. It may be used for technology evaluation from the wafer incoming inspection stage to the final device.

TABLE III.

RESULTS OF DC CHARACTERIZATION OF DEVICES PRODUCED ON W1 AND W2

Wafer	**Idss [mA/mm]**	**Vp [V]**
W1	304	-0.87
W2	258	-0.72

CONCLUSIONS

In conclusion, GaN/AlGaN HEMT, MHEMT and PHEMT epitaxial structures have been characterized by SPS. Effects of $?_{top}$?, $?_{bot}$ and Q_{sur} on SPV spectra were found, using numerical simulations. A complete empirical model providing doping levels has been developed. The universality of the model for characterization of HEMT structures of various material compositions is shown. The capability of characterization using SPS to predict the final device performance has been demonstrated for MHEMT structures.

ACKNOWLEDGEMENTS

The authors would like to thank A. Fainburn and S.Caster that helped take the measurements.

REFERENCES

[1] J.Bernat, et al, 2002 GaAs IC Symposium Technical Digest, p.243.
[2] Y. Yamashita, et al, IEEE Electron Device Letters, 22, 367, (2001).
[3] S. Bollaert, et al, Electronics Letters , 38 ,389 (2002).
[4] S.A. Brown and J.M. Carroll, 2000 GaAS IC Symposium Technical Digest, p.223.
[5] K. Radhakrisnan, et al , Microelectronic Engineering, 51-52, 441 (2000).
[6] C.Y. Fang, et al, Appl. Phys. Lett., 80, 4558 (2002).
[7] F.H. Pollak , Materials Science and Engineering, B80, 178 (2001).
[8] A. Torabi, et al, J. Vac. Sci . Technol. B 20(3), 1234 (2002).
[9] Y.T.Cheng, et al, Physica E, 14, 313 (2002).
[10] L. Kronik and Y. Shapira, Surface & Interface Analysis, 31, 954 (2001).
[11] B. Mishori, et al , Appl. Phys. Lett., 73, 650 (1998).
[12] N. Bachrach-Ashkenasy, et al, Appl. Phys. Lett., 68, 879, (1996).
[13] N. Ashkenasy, et al , J. Appl. Phys., 83, 1146 (1998).
[14] N. Ashkenasy, et al, J. Appl. Phys., 86, 6902 (1999).
[15] S.Solodky, et al, J. Appl. Phys., 88, 6775 (2000).
[16] Y. H. Zhang and K. Ploog, Phys. Rev. B, 45, 14069 (1992).
[17] B.M. Green, K.K. et al, IEEE Electron Device Letters, 21, 268, (2000).
[18] Ngyen et al, Proceddings IEEE, 80, 494 (1992).